

Curved Reconstruction along the Anterior Optic Pathway

Suzanne A. Gronemeyer, James W. Langston, and Jacob Abraham

Summary: Curved reconstruction of a three-dimensional data set along the anterior optic pathway improves visibility of the optic nerves and chiasm and facilitates comparison between the two nerves. Curved reconstruction reveals three patterns in patients with masses of the anterior optic pathway. Retrobulbar buckling of the optic nerve into a “periscope” configuration is observed in some patients.

We developed a useful technique that enables visualization of the anterior optic pathway in one image. This “frog-eye” view gives the radiologist an improved perspective on masses of the optic nerve and chiasm, thus facilitating comparison of the nerves and visualization of increased perineural fluid. We find it to be a useful complement to standard imaging techniques.

Methods

A three-dimensional image set was obtained using a magnetization-prepared rapid acquisition gradient-echo (MP-RAGE) sequence (1, 2). The image set was obtained without intravenous contrast material to minimize motion artifacts from flowing blood. The imaging parameters were 13/5/1 (repetition time/echo time/excitations) with a 15° flip angle and an inversion time of 500. The sagittal slab was 160-mm thick with 128 partitions, yielding a partition thickness of 1.25 mm. A 200-mm field of view was used with a 256 × 256 matrix to obtain in-plane resolution of 0.8 × 0.8 mm. Image acquisition time was 9 minutes 17 seconds. The MP-RAGE sequence provided as part of the scanner software was modified to reduce truncation artifacts (3).

An oblique transverse reconstruction section 30- to 40-mm thick containing the optic nerves and chiasm was selected (Fig 1A). On the oblique transverse image, a curved reconstruction line was drawn beginning in front of the lens of one eye back through the optic nerve, through the chiasm, and out through the other optic nerve to the lens of the contralateral eye (Fig 1B). Reconstruction along this line yields the frog-eye perspective (Fig 1C). Since conventional views are used to evaluate the chiasm per se, the reconstruction line need not pass consistently through the center of the chiasm, but should be drawn to yield good visualization of the entry of the optic nerves into the chiasm.

Initially, frequency encoding was done in the normal craniocaudal direction, which produces a marked craniocaudal chemical shift (4, 5) of the nerve and cerebrospinal fluid space with respect to orbital fat (Fig 2A) and accentuates dilatation of the

optic nerve sheath. On later patients, frequency encoding was done in the anteroposterior direction to eliminate craniocaudal chemical-shift displacement of the optic nerve and perineural fluid with respect to surrounding retrobulbar fat (Fig 2B).

Results

With the frog-eye view, both optic nerves and the chiasm can be examined in one curved-plane image, facilitating comparison of the two nerves. We observed three mass patterns in patients with anterior optic pathway masses: an enlarged chiasm and/or intracranial optic nerve(s) with normal orbital optic nerves (Fig 1C); a normal chiasm and intracranial optic nerves with enlarged orbital optic nerve(s) (Fig 2); and an enlarged chiasm and intracranial and orbital optic nerves (Figs 3 and 4).

Enlargement of the optic nerve in all three dimensions in patients with neurofibromatosis type 1 (NF1) can produce longitudinal buckling, which causes a “periscope” appearance on the frog-eye view (Figs 3 and 4A). The enlarged cerebrospinal fluid space around the optic nerve often observed in these patients is particularly well appreciated on the frog-eye view (Figs 2, 3, and 4A). Optic nerve buckling combined with enlarged perineural space produces a “doughnut” sign on transverse images (Fig 4B). Normal optic nerves usually follow a downward-curving bow between the optic chiasm and the globe, as seen in the normal left nerve in the patient in Figure 5. When the nerves elongate in patients, they usually buckle downward just behind the globe, which is the largest part of the intraconal space. We postulate that the nerves buckle downward as an exaggeration of their normal bowed shape.

Conclusion

Although the three patterns we illustrate can be seen adequately with standard imaging planes (axial, sagittal, and coronal), we find the frog-eye view helpful in assessing the optic nerve component of anterior optic pathway masses. It is particularly well suited for visualizing the retrobulbar periscope buckling of the optic nerve caused by nerve elongation. Although we have not compared this technique prospectively with our standard imaging protocol, we find it helpful in some patients.

Acknowledgments

We thank Mark Brown, Charles Collins, and Orlando Simionetti of Siemens Medical Systems for help in optimizing the

Received October 18, 1996; accepted after revision February 19, 1997.

Supported in part by the National Cancer Institute, Cancer Center Support CORE grant P30CA21765, and by the American Lebanese Syrian Associated Charities (ALSAC).

From the Department of Diagnostic Imaging, St Jude Children’s Research Hospital, Memphis, (S.A.G., J.W.L., J.A.), and the Department of Radiology (S.A.G., J.W.L.), University of Tennessee, Memphis.

Address reprint requests to Suzanne A. Gronemeyer, PhD, Department of Diagnostic Imaging, St Jude Children’s Research Hospital, 332 N Lauderdale, Memphis, TN 38105.

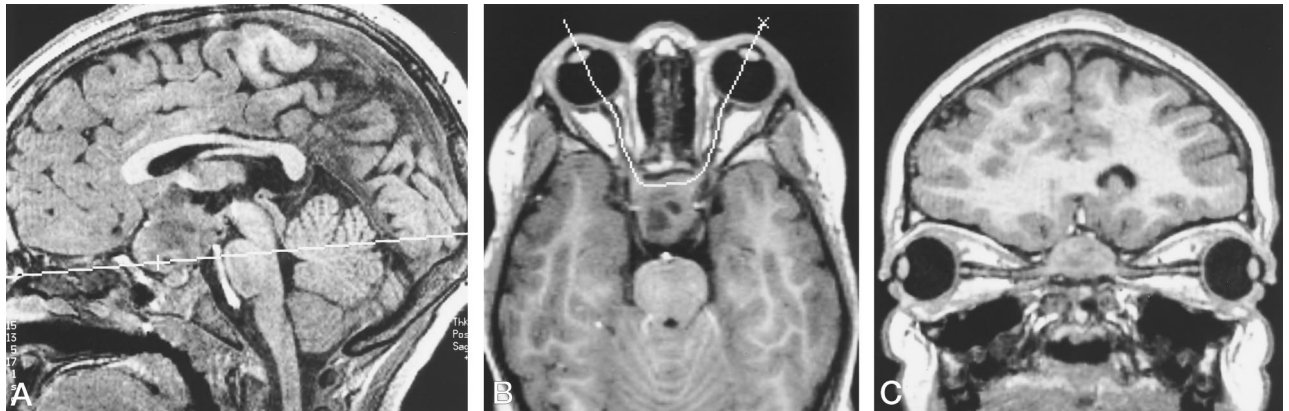


FIG 1. Three-year-old girl with glioma of the optic pathway.

A, Sagittal 3-D MP-RAGE image with plane selected for oblique transverse reconstruction.

B, Reconstructed oblique 40-mm-thick transverse image with curved line through the complete anterior optic pathway selected for frog-eye reconstruction.

C, Reconstructed frog-eye view of the entire anterior optic pathway reveals an enlarged chiasm with normal orbital optic nerves.

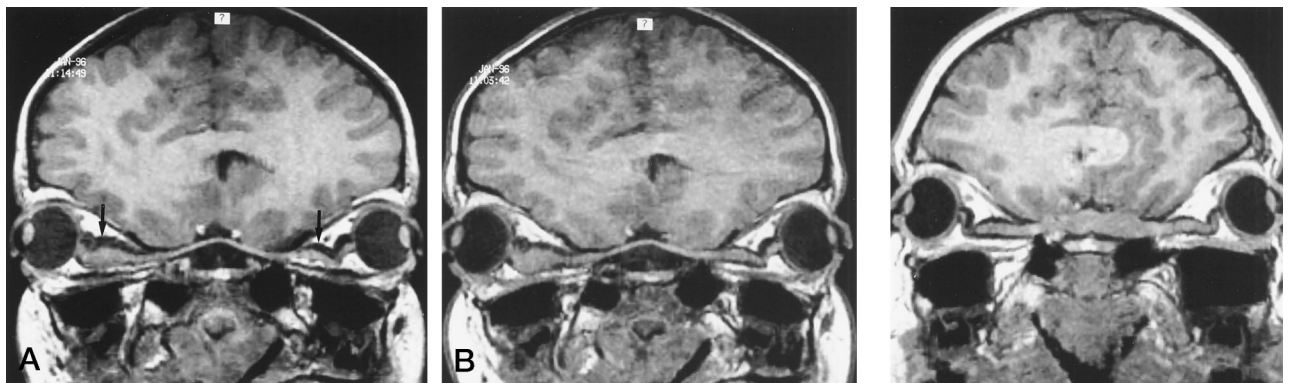


FIG 2. Six-year-old boy with NF1.

A, Frequency encoding is craniocaudal. Notice the marked dorsoventral chemical shift (arrows) of the nerves and cerebrospinal fluid space with respect to orbital fat, which accentuates dilatation of the optic nerve sheath.

B, Frequency encoding is anteroposterior. The effect of the chemical shift is minimized. A normal chiasm and intracranial optic nerves with enlarged orbital optic nerves are well seen.

FIG 3. Nine-year old girl with NF1 and an optic pathway glioma. Frog-eye view shows enlarged chiasm and intracranial and orbital optic nerves.

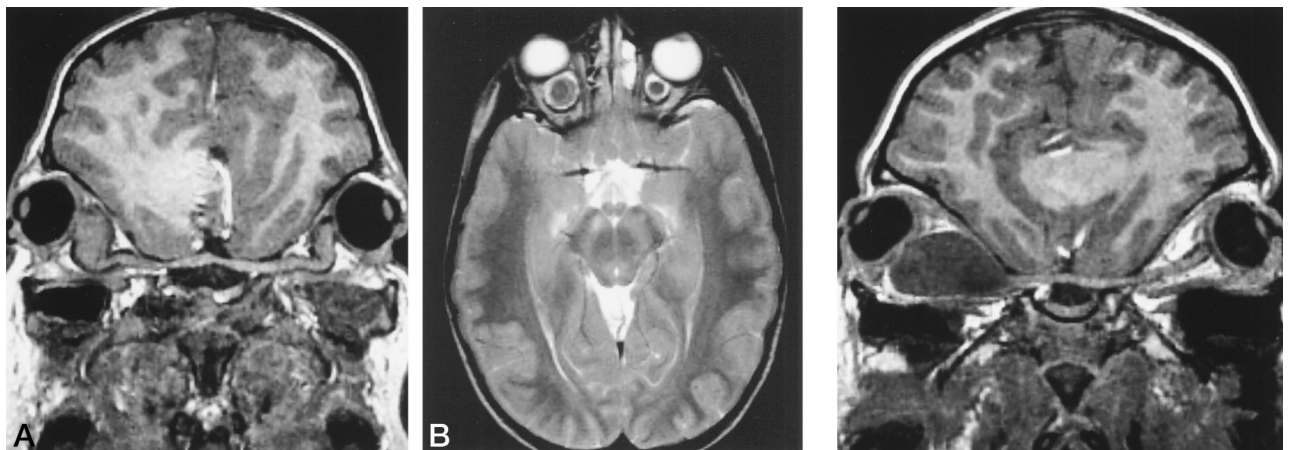


FIG 4. Four-year-old girl with NF1 and an optic pathway glioma.

A, Enlarged chiasm and intracranial and orbital optic nerves. Enlargement of the optic nerve in all dimensions has produced a longitudinal buckling and resultant periscope appearance on the frog-eye view.

B, A cross-section through the upwardly turned and buckled optic nerves causes a doughnut appearance.

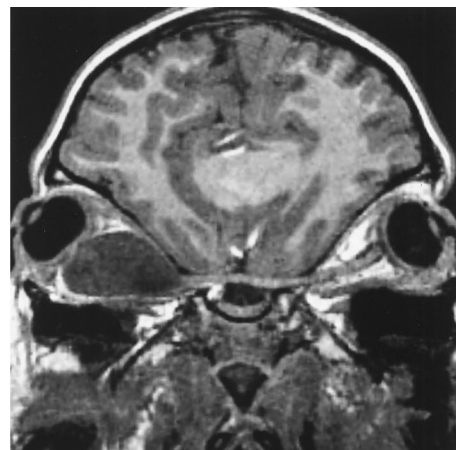


FIG 5. Seven-year-old boy with juvenile pilocytic astrocytoma of the right optic nerve. The normal left optic nerve forms a downward bow between the optic chiasm and the globe.

3-D MP-RAGE sequence. Francine Kim provided helpful comments on the manuscript.

References

1. Mugler JP, Brookeman JR. **Three-dimensional magnetization-prepared rapid gradient-echo imaging (3D MP RAGE)**. *Magn Reson Med* 1990;15:152-157
2. Mugler JP, Brookeman JR. **Rapid three-dimensional T1-weighted MR imaging with the MP-RAGE sequence**. *J Magn Reson Imaging* 1991;1:561-567
3. Wood ML, Henkelman RM. **Truncation artifacts in magnetic resonance imaging**. *Magn Reson Med* 1985;2:517-526
4. Soila KP, Viamonte M Jr, Starewicz PM. **Chemical shift misregistration effect in magnetic resonance imaging**. *Radiology* 1984;153:819-820
5. Daniels DL, Kneeland JB, Shimakawa A, et al. **MR imaging of the optic nerve and sheath: correcting the chemical shift misregistration effect**. *AJNR Am J Neuroradiol* 1986;7:249-253